DOI: 10.1002/ejic.200900310

Synthesis and Photophysical Properties of 3,8-Disubstituted 1,10-Phenanthrolines and Their Ruthenium(II) Complexes

Michael Karnahl,[a] Sven Krieck,[a] Helmar Görls,[a] Stefanie Tschierlei,[b] Michael Schmitt,[b] Jürgen Popp,*[b,c][‡] Daniel Chartrand,[d] Garry S. Hanan,[d] Robert Groarke,[e] Johannes G. Vos,[e] and Sven Rau*[a,f][‡‡]

Keywords: Phenanthroline / Ruthenium / Pd catalysis / Luminescence / Resonance Raman spectroscopy

The palladium-catalysed cross-coupling reaction between 3,8-dibromo-1,10-phenanthroline with phenylacetylene or 3,5-bis(trifluoromethyl)phenylboronic acid gives good yields of the 3,8-disubstituted products. These 1,10-phenanthroline derivatives are used for the formation of novel ruthenium complexes of the type $[(tbbpy)_2Ru(phenR_2)]^{2+}$ [where tbbpy = 4,4′-di-*tert*-butyl-2,2′-bipyridine, phen = 1,10-phenanthroline, R represents the substituents at the 3,8 positions with bromine, phenylacetylene or 3,5-bis(trifluoromethyl)-phenyl]. All compounds are completely characterised by NMR and UV/Vis spectroscopy, MS, electrochemical measurements and Raman and resonance Raman spectroscopy. The photophysical properties indicate a strong influence of the substitution of the phenanthroline ligand on the absorption, emission and Raman properties. With resonance Raman spectroscopy the localisation of the singlet metal-to-ligand charge-transfer (^{1}MLCT) excited state is determined. The solid-state structures of 3,8-dibromo-1,10-phenanthroline ($phenBr_2$) and the corresponding ruthenium complex $[(tbbpy)_2Ru(phenBr_2)]^{2+}$ and a structural motif of $[(tbbpy)_2$-Ru{phen-3,8-bis[3,5-bis(trifluoromethyl)phenyl]}$]^{2+}$ are also reported.

Introduction

Ruthenium coordination compounds, based on polypyridine ligands, play a central role in the design of luminescent and redox-active assemblies. Therefore, the development of photochemical molecular devices (PMD)[1–3] with ligands of the 1,10-phenanthroline type (phen) has been investigated extensively.[4] It is of fundamental importance to possess a variety of synthetic methods to obtain derivatives of the phen ligand in order to be able to introduce substituents that can tune the photophysical properties of its transition-metal complexes.[5–8] Phenanthrolines are an interesting scaffold and are very versatile building blocks as they offer several positions that can be manipulated (Figure 1).[9–15]

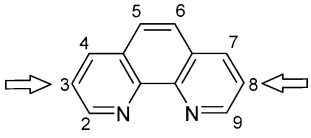

Figure 1. Structure of 1,10-phenanthroline (phen) and the applied numbering scheme. The two arrows mark the desired 3,8 positions.

For example, oxidation of phen at the 5,6 positions leads to the corresponding 1,10-phenanthroline-5,6-dione, which is an important building block for the construction of oligopyridophenazines, such as di- and tetrapyridophenazine ligands.[16–20] Their ruthenium complexes may be used as luminescent probes for DNA (DNA sensors)[21,22] or light-harvesting centres for intramolecular photocatalytic hydrogen formation.[23–27] In this contribution, we wish to report novel methods for the introduction of substitution at the 3 and 8 positions of the 1,10-phenanthroline ring (Figure 1). It is important to note that introduction of substituents at the 2,9 positions can render the corresponding ruthenium complexes photolabile,[13,15,18,28,29] while substitution at the 3,8 positions will influence the photophysical properties without interfering with the coordination sphere.[10,30]

[a] Institut für Anorganische und Analytische Chemie, Friedrich-Schiller-Universität, August-Bebel-Str. 2, 07743 Jena, Germany
[b] Institut für Physikalische Chemie, Friedrich-Schiller-Universität, Helmholzweg 4, 07743 Jena, Germany
Fax: +49-3641-948302
E-mail: juergen.popp@uni-jena.de
[c] Institute of Photonic Technology Jena e.V., Albert-Einstein-Straße 9, 07749 Jena, Germany
[d] Département de Chimie, Université de Montréal, 2900 Edouard-Montpetit, Montréal, Québec H3T-1J4, Canada
[e] Solar Energy Conversion SRC, School of Chemical Sciences, Dublin City University, Dublin 9, Ireland
[f] Department for Chemistry and Pharmacy, Friedrich-Alexander-University Erlangen-Nürnberg, Egerlandstraße 1, 91058 Erlangen, Germany
Fax: +49-9131-8527367
E-mail: sven.rau@chemie.uni-erlangen.de
[‡] Correspondence for Raman and resonance Raman spectra.
[‡‡] Correspondence for the synthesis and the materials.

Furthermore, 1,10-phenanthroline ligands substituted at the 4,7 positions are already known and applied in ruthenium(II) complexes as luminescent sensors for oxygen.[31,32]

The introduction of bromine functions into the ligand framework is especially interesting as they allow the application of palladium-catalysed Suzuki[33–36] and Sonogashira[37] cross-coupling reactions thus enabling the introduction of phenyl or alkynyl derivatives at predesignated positions. In addition, nucleophilic substitution at these positions allows the introduction of alkoxides[12] and amino acids.[38] Recently we reported that these reactions can also be employed for 3,5,6,8-tetrabromophenanthroline ($phenBr_4$), where a stronger influence of the alkynyl moiety than that of the aryl moiety on the photophysical properties, such as absorption and emission maxima, was observed.[12,14]

The combination of electron-rich bipyridine ligands, such as tbbpy, with electron-deficient bipyridine ligands, like 4,4′-bis(methoxycarbonyl)-2,2′-bipyridine, leads to interesting photophysical properties of the corresponding complexes such as excitation-wavelength-dependent switches of the localisation of the singlet metal-to-ligand charge-transfer state.[39] The introduction of alkynyl- or aryl groups into the phenanthroline frames at the 3,8 positions leads to an expansion of the conjugated π system, which lowers the energy of the phenanthroline-based excited state. Here, we present the synthesis, characterisation and photophysical properties of three different mononuclear ruthenium polypyridine complexes based on 3,8-disubstituted 1,10-phenanthroline ligands.

Results and Discussion

Synthesis

The desired compounds were synthesised according to Schemes 1 and 2. 3,8-Dibromo-1,10-phenanthroline, **L2**, was obtained by using literature methods[8] starting from 1,10-phenanthroline, **L1**. The solid-state structure of **L2** is depicted in Figure 2.

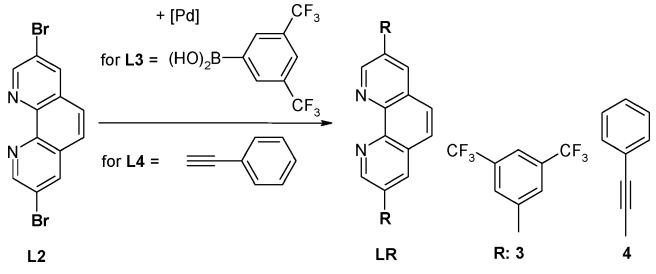

Scheme 1. Synthesis and naming of disubstituted phenanthroline ligands.

The two bromine functions in **L2** can be modified by using different types of palladium-catalysed carbon–carbon bond-forming reactions. Reaction of **L2** with 2 equiv. 3,5-bis(trifluoromethyl)phenylboronic acid under Suzuki[33,36] cross-coupling conditions (in thf, Cs_2CO_3, 80 °C, 3 d) gives

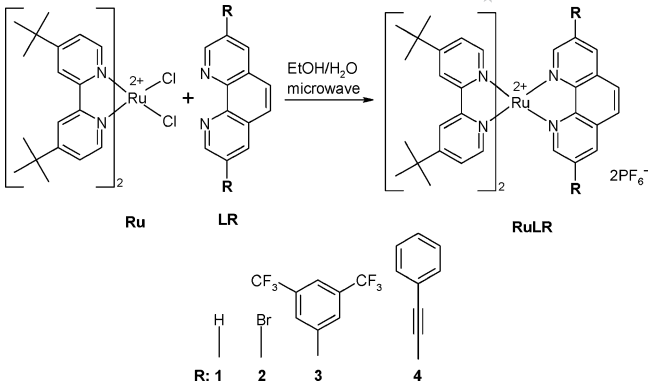

Scheme 2. Synthesis and labelling of the presented ruthenium complexes.

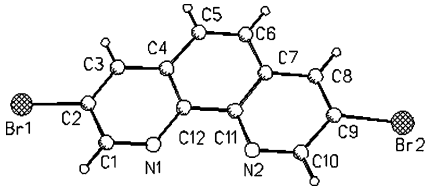

Figure 2. Solid-state structure and numbering of **L2**, relevant bond lengths and angles are given in Table 1, solvent molecules are omitted for clarity.

3,8-bis[{3,5-bis(trifluoromethyl)}phenyl]-1,10-phenanthroline [**L3**, $phen(tfmp)_2$] in very good yields. The combination of $Pd_2(dba)_3$ and S-Phos (in the ratio of 1:2) was found to be the most effective catalytic system for preparation of **L3** (yield = 95%). The alternative use of $Pd(PPh_3)_4$ and Na_2CO_3 under comparable reaction conditions resulted in incomplete conversion and diminished yields of only 25%.

L2 can also be transformed into the 3,8-bis(arylethynyl)-1,10-phenanthroline **L4** by using an ultrasonic activated Sonogashira coupling reaction.[37] It has to be mentioned that the application of sonication is essential for the effective palladium-catalysed C–C bond formation.[10,37] Thus, the reaction mixture was sonicated at 40 °C under argon atmosphere for 8 h before the suspension was heated to 60 °C for 1 d. After workup and purification by column chromatography, it was possible to isolate 3,8-bis(phenylacetylene)-1,10-phenanthroline [**L4**, $phen(phac)_2$] in yields of 81% (Scheme 1).

NMR measurements and mass spectra are all in good agreement with the proposed structure. The regioselective addition of two arylethynyl groups in the 3,8 positions leads to an increased conjugated aromatic system, that has not only an influence on the solubility, it further affects the photophysical properties, as discussed later.

The coordination of these new ligands to the $[(tbbpy)_2Ru]^{2+}$ core was accomplished by using microwave-assisted reaction conditions with short reaction times of only two hours, to afford the target complexes in yields of above 70%. Furthermore, purification from side products by column chromatography was not necessary as simple recrystallisation sufficed.

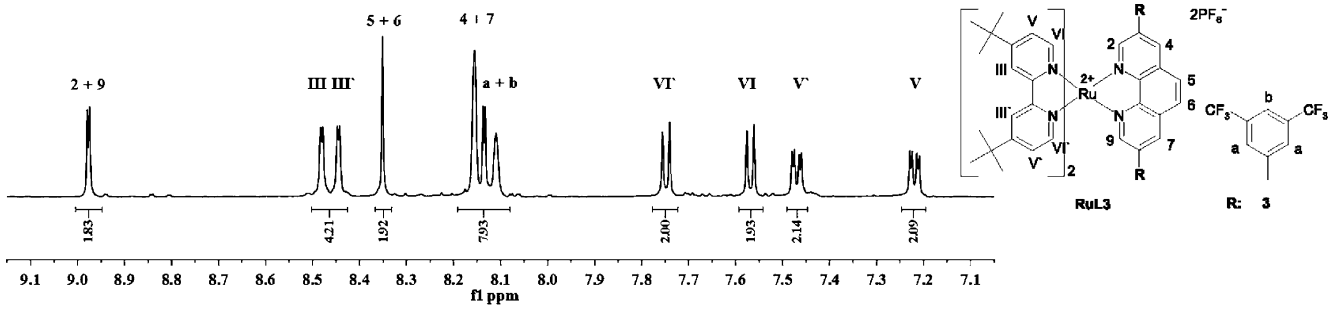

Figure 3. ^{1}H NMR spectrum (400 MHz, 300 K) of Ru**L3** in CD_3CN and the assignment of the NMR values.

The structural characterisation of the new ruthenium complexes was performed with multidimensional NMR methods (H,H-COSY), MS (ESI), UV/Vis, emission and Raman spectroscopy and, wherever possible, X-ray analysis. The results of the investigation of the complexes Ru**L2**–Ru**L4** by ESI mass spectroscopy always confirm the composition of the complexes. In each case the $[M - 1PF_6]^+$ and the $[(M - 2PF_6)/2]^+$ peak can be assigned to the corresponding fragment with matching isotopic pattern. One representative example for a ^{1}H NMR spectrum is given in Figure 3. The signals corresponding to the hydrogen atoms of the phenanthroline ligand of Ru**L3** are marked with numbers. As expected, the phen moiety provides three different proton signals with a characteristic shape (two doublets and one singlet, marked with Latin numbers) and equal peak areas. This ^{1}H NMR pattern indicates the formation of a symmetrical octahedral complex, which is in agreement with the crystallographic characterisation (Figure 5).

In addition to the characterisation of the novel mononuclear compounds Ru**L2**–Ru**L4** by means of NMR spectroscopy, the X-ray structures of Ru**L2** and Ru**L3** are depicted in Figures 4 and 5. The structural analysis of Ru**L2** indicates a conventional octahedral coordination environment around the ruthenium centre, which is common for these classes of coordination compounds.[12] A detailed comparison of the results of the X-ray crystallographic analysis (Table 1) reveals only slight differences between **L2** and the corresponding ruthenium complex Ru**L2**. All selected bond lengths and angles are in the same range, and the phenanthroline frame is nearly ideally planar (deviation from planarity is 9 pm). There are also no significant differences in the bond lengths and angles when Ru**L1** and Ru**L2** are compared. The same trend can be found for the analogous tetrabromo-substituted ruthenium complex $RuBr_4$ ($[(tbbpy)_2Ru(phenBr_4)]^{2+}$), with four bromine functions at the positions 3, 5, 6 and 8.[12] The Ru–N bond lengths (depicted in Table 1) are in the same range as those found for related Ru complexes.[12] Hence, it is obvious that bromine substitution (neither its position nor the number) has no significant influence on the solid-state structure.

The structural motif of Ru**L3** is depicted in Figure 5, which was obtained by crystallisation from an acetone/water mixture. The ruthenium centre is octahedrally surrounded by two tbbpy chelate ligands and one 3,8-bis[{3,5-bis(trifluoromethyl)}phenyl]-1,10-phenanthroline ligand,

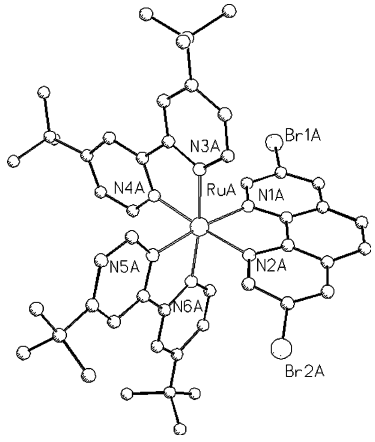

Figure 4. Solid-state structure of Ru**L2**. Hydrogen atoms, PF_6^- anions and solvent molecules are omitted for clarity.

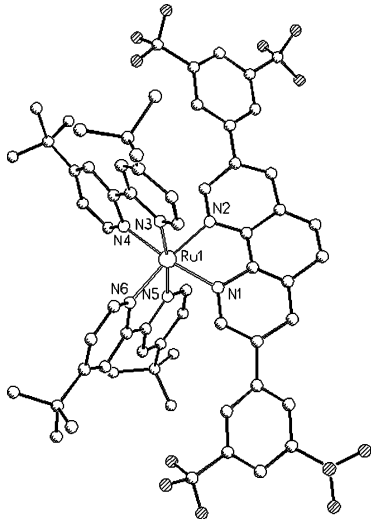

Figure 5. Solid-state structural motif of Ru**L3**. Hydrogen atoms, PF_6^- anions and solvent molecules are omitted for clarity.

where the phenyl rings are twisted out of the phenanthroline plane. This is caused by rotation of the aromatic rings to avoid steric strain, which results in a potential lack of delocalisation of the conjugated π system. Unfortunately, the quality of this structural motif is not high enough for a more detailed discussion of the bond lengths and bond angles.

Table 1. Bond lengths [pm] and angles [°] of **L2**, Ru**L1** and Ru**L2**. For atom numbering see also Figure 2.

	L2	Ru**L1**[a]	Ru**L2**	$RuBr_4$[a]
Br1–C2	189.4±2.4	–	188.6±2.1	189.1±1.8
Br2–C9	187.9±2.4	–	189.9±2.1	187.7±1.8
C1–N1	131.4±3.0	135.7±2.7	135.5±2.4	133.4±2.1
C3–C4	142.0±3.3	139.4±4.5	139.0±3.3	140.7±2.7
Ru1–N1	–	206.1±1.5	204.0±1.5	204.6±1.5
Ru1–N2	–	205.6±1.5	205.8±1.5	206.0±1.5
Ru1–N3	–	205.3±1.2	204.9±1.2	206.4±1.5
Ru1–N4	–	205.5±1.2	204.8±1.5	205.2±1.5
Br1–C2–C3	121.2±1.8	–	120.4±1.5	122.2±1.5
C3–C4–C5	122.3±2.1	126.1±3.0	124.0±2.1	125.0±1.8
C1–N1–C12	118.9±2.1	117.6±1.8	118.5±0.9	118.6±1.5
N1–Ru1–N2	–	79.9±0.6	79.7±0.6	79.3±0.6
N1–Ru1–N3	–	91.2±0.5	87.8±0.5	91.8±0.6
N3–Ru1–N4	–	77.9±0.5	78.8±0.5	78.2±0.6

[a] The data of Ru**L1** and $RuBr_4$ are taken from Rau et al.[12] and are given for comparison.

Electrochemistry

The electrochemical measurements were carried out in anhydrous and nitrogen-purged acetonitrile with 0.1 M tetrabutylammonium tetrafluoroborate as supporting electrolyte. The resulting cyclic voltammograms of Ru**L1**–Ru**L4** are consistent with a metal-based reversible oxidation step and several ligand-based reduction steps, which are presented in Table 2. In comparison to the unsubstituted phenanthroline ligand in Ru**L1** [$E_{ox}^{Ru(II/III)}$ = 0.79 V], all the oxidation potentials of the Ru^{II}/Ru^{III} couple in Ru**L2**–Ru**L4** lie towards more positive values, but they are only slightly affected by the substitution pattern. This suggests that the introduction of substituents has a comparatively moderate influence on the metal-based ground state. The most pronounced of the oxidation potentials of the Ru^{II}/Ru^{III} couple, with a difference of 90 mV, is for Ru**L2**, which clearly shows that the two bromine substituents decrease the electron density at the metal centre.

Table 2. Electrochemical data: half-wave potentials E [V] (vs. Fc/Fc^+).

Compound	$E_{ox}^{Ru(II/III)}$	E_{red}^{I}	E_{red}^{II}	E_{red}^{III}	E_{red}^{IV}
Ru**L1**	0.79	–1.79	–1.99	–2.26	–
Ru**L2**	0.88	–1.53	–2.02	–2.27	–
Ru**L3**	0.81	–1.69	–1.95	–2.21	–2.56
Ru**L4**	0.85	–1.46	–2.02	–2.30	–

The first reduction processes of Ru**L2**, Ru**L3** and Ru**L4** occur at markedly less cathodic potentials relative to that of Ru**L1**, with a shift of 0.35 V for Ru**L2** and 0.33 V for Ru**L4**, which arises because of the more pronounced π acceptance by the substituted phen ligand. The second and third reductions at around –2.0 V and –2.3 V are ascribable to the stepwise one-electron tbbpy-based reductions. These values are in good agreement with the potentials obtained for the recently described systems Ru**L1**.[12,14] The complex Ru**L3** shows an additional reduction step at –2.56 V, which is in accordance to reported complexes with a tetrasubstituted phenanthroline moiety $[(tbbpy)_2Ru(phenBr_4)](PF_6)_2$ and $[(tbbpy)_2Ru\{phen(Ph\text{-}4\text{-}tBu)_4\}](PF_6)_2$.[12,14] In conclusion, Ru**L2** with the bromine substitution in positions 3 and 8 exhibits clear differences in its redox potentials relative to the unsubstituted complex Ru**L1**. Therefore, it would be interesting if differences can also be found in the photophysical properties, which are discussed below.

Electronic Properties

The clear influence of the different substituents on the absorption and emission properties, as well as on the luminescence lifetimes, is listed in Table 3. The absorption spectra of **L1**–**L4** dissolved in dichloromethane are shown in Figure 6. All four ligands display two absorption maxima, independent of their substitution, in the wavelength range from 230 to 400 nm. The ligands **L2**–**L4** exhibit a considerable redshift of the π–π* transitions, and an increased intensity of these two bands relative to 1,10-phenanthroline, **L1**. For **L1**, the difference between these two absorption bands at 233 and 265 nm is 32 nm. A comparable behaviour can be found for the absorption maxima of the ligand **L2** with a bathochromic shift from 233 to 246 nm and from 265 nm to 275 nm relative to the unsubstituted ligand **L1**, and for **L3**, the maxima occur at 278 and 321 nm. These spectroscopic properties are comparable to related 3,5,6,8-tetraphenyl-1,10-phenanthroline ligands.[14] Substitution with phenylacetylene (**L4**) results in a significant variation in the absorption properties as discussed by Tzalis et al.[10] These absorption maxima are located at 284 and 347 nm with a shoulder at 359 nm.[10] It seems that the phenylacetylene substituents have the strongest influence on the π system of the phenanthroline moiety.

An influence of the substitution pattern on the emission features of **L1**–**L4** dissolved in dichloromethane, excited at their long-wavelength absorption maxima, is also clearly visible. The emission maxima display a significant redshift on going from **L1** to **L4** as shown in Table 3. The emission maxima for **L1** and **L2** are located at 365 and 368 nm, respectively, and a bathochromic shift from 365 to 391 and 414 nm occurs for the emission of **L3** and **L4**, respectively. Similar redshifts of the emission wavelength have been ob-

Table 3. Absorption, emission properties, lifetimes and quantum yields of the 1,10-phenanthroline ligands **L1**–**L4** and the corresponding ruthenium complexes Ru**L1**–Ru**L4** dissolved in dichloromethane.

Compound	Absorption λ_{max} [nm] ($\varepsilon/10^3$ M^{-1} cm^{-1})	Emission λ_{max}[a] [nm]	Lifetime, τ[b] [ns]	Quantum yield, ϕ
L1	233 (33), 265 (32)	365	–	<0.01
L2	246 (52), 275 (42)	368	–	<0.01
L3	278 (37), 321 (23)	391	–	0.03
L4	284 (51), 347 (55), 359 (51)	414	–	0.47
Ru**L1**	267 (64), 288 (69), 426 (16), 455 (19)	602	272	0.03
Ru**L2**	282 (59), 289 (83), 440 (19), 470 (16)	638	525	0.05
Ru**L3**	286 (98), 322 (31), 441(12), 485 (11)	652	480	0.05
Ru**L4**	287 (109), 371 (68), 440 (19), 502 (11)	657	591	0.05

[a] **L1**–**L4**: λ_{exc} at the long-wavelength maximum, Ru**L1**–Ru**L4**: λ_{exc} = 440 nm. [b] λ_{exc} = 337 nm.

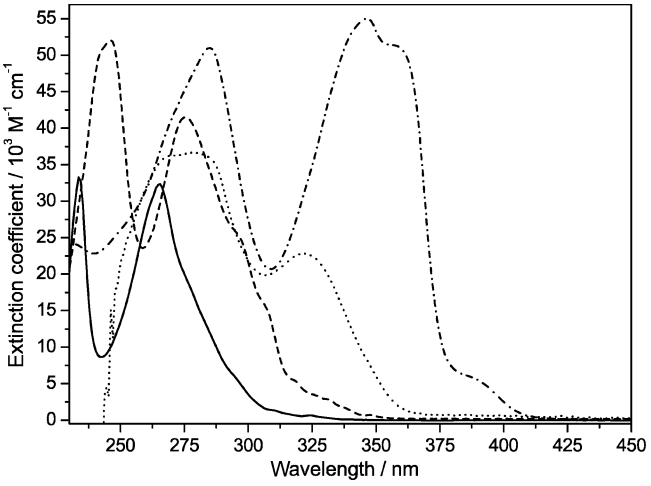

Figure 6. Absorption spectra of **L1** (solid), **L2** (dashed), **L3** (dotted), **L4** (dash–dotted) dissolved in dichloromethane.

served in fourfold-substituted phenanthroline ligands.[14] The Stokes shift decreases in the order **L1** (1.28 eV), **L2** (1.14 eV), **L3** (0.69 eV) and **L4** (0.46 eV).

On the basis of these investigations, it is apparent that substitution at the 3,8 positions of the 1,10-phenanthroline ligand has a pronounced influence on the photophysical properties of phenanthroline ligands. The strongest effect is observed for the alkynyl substituent, which likely correlates with the most increased delocalisation of the conjugated π system.[10]

All four complexes Ru**L1**–Ru**L4** dissolved in dichloromethane exhibit absorption properties that are common for the class of ruthenium polypyridine compounds (Figure 7).[40] The absorption spectra of Ru**L1** and Ru**L2** are very similar. Ru**L1** exhibits four absorption maxima at 267, 288, 426 and 455 nm. The maxima at 267 and 288 nm can be assigned to ligand-centred π–π* transitions of **L1** and 4,4′-bis(*tert*-butyl)-2,2′-bipyridine (tbbpy), respectively.[10] Furthermore, the two maxima at 426 and 455 nm correlate to metal-to-ligand charge-transfer (^{1}MLCT) transitions between the ruthenium ion and the coordinated ligands.[40] The complex Ru**L2** displays very similar properties; for instance, a notable shift in the lowest-energy absorption band from 426 and 455 nm for Ru**L1** to 440 and 470 nm for Ru**L2** is observed. This shift is very comparable with data obtained for the $[Ru(tbbpy)_2(phenBr_4)]^{2+}$, where the bromine groups are located at the 3, 5, 6 and 8 positions,[14] and for the complex $[Ru(bpy)_2(phenBr_2)]^{2+}$ without *tert*-butyl groups.[30] A further bathochromic shift of the absorption occurs for Ru**L3**. The band maxima located at 286 and 322 nm are assigned to ligand-centred π–π* transitions of tbbpy and **L3**, respectively. The other two maxima at 441 and 486 nm can be assigned to electronic transitions between orbitals of the ruthenium and the π* orbitals either tbbpy or **L3**. Comparable properties have been observed for complexes with different fourfold phenyl substitutions at the 3, 5, 6 and 8 positions.[14] The absorption properties of Ru**L4** differ from the other presented coordination compounds. A particular feature is the band at 371 nm for Ru**L4**, which can be assigned to the ligand-centred π–π* transition of **L4** (by comparison, the absorption of the unbound ligand **L4** occurs at 359 nm, Figure 6). Furthermore a bathochromic shift of the absorption band with the lowest energy is clearly visible, because the absorption maximum of this ^{1}MLCT transition is located at 502 nm with a red-shift of 47 nm relative to the unsubstituted complex Ru**L1** and 16 nm to Ru**L3**. Very similar absorption properties have been reported for a ruthenium complex with a 3,5,6,8-tetrakis[(triisopropylsilyl)acetylene]-1,10-phenanthroline ligand and for a structurally related osmium complex with a

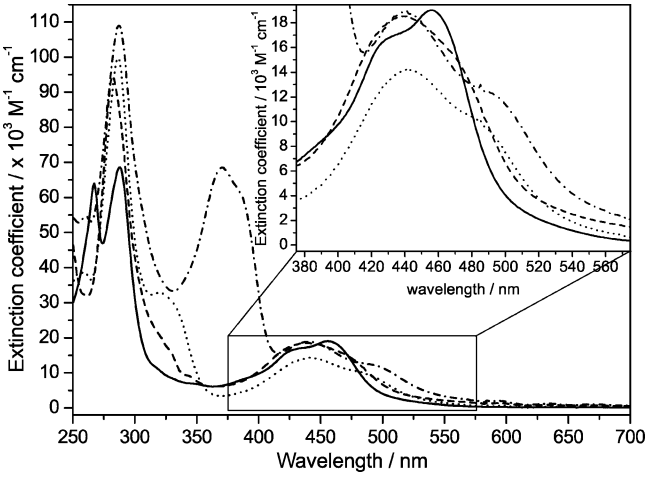

Figure 7. Absorption spectra of Ru**L1** (solid), Ru**L2** (dashed), Ru**L3** (dotted) and Ru**L4** (dash–dotted) in dichloromethane; an enlargement of the MLCT region is depicted in the inset.

3,8-bis(phenylacetylene)-1,10-phenanthroline ligand where the absorption maxima are shown at 505[41] and 497 nm,[42] respectively.

The emission maxima and emission lifetimes of complexes Ru**L1**–Ru**L4** dissolved in dichloromethane were also investigated (Table 3). When the data obtained for the substituted complexes are compared with that of Ru**L1**, a bathochromic shift of the emission wavelengths from 602 nm (Ru**L1**) to 638 nm (Ru**L2**), 652 nm (Ru**L3**) and 657 nm (Ru**L4**) is observed. The largest bathochromic shifts of the emission maxima appear for Ru**L3** and Ru**L4**, which indicates that the phenyl and phenylacetylene groups have the strongest influence on the π system of the phenanthroline system. Similar bathochromic shifts of the emission maxima have been observed for a ruthenium complex with a 3,5,6,8-tetrakis[(triisopropylsilyl)acetylene]-1,10-phenanthroline ligand with a maximum at 692 nm.[41] For complexes with a dual phenylacetylene substitution at the 4 and 7 positions, similar properties with an emission maximum at 672 nm have been observed.[43] The analysis of the luminescence lifetimes, recorded in aerated dichloromethane with an excitation wavelength of 337 nm, shows that all substituted complexes display significantly longer lifetimes than the unsubstituted Ru**L1**. However, the type of substitution has no significant influence on the emission lifetime. This surprising finding might be explained by the combined effect of the substitution at the 3,8 positions, together with the deactivating effect of the large substituents, which might offer additional nonradiative relaxation pathways.

The quantum yields of the emission for all complexes are in the range expected for ruthenium polypyridyl complexes. The bromine substituent seems to lower the quantum yield to some extent. In summary, the substitution in the 3,8 positions of the non-coordinated and the coordinated 1,10-phenanthroline ligand has a considerable influence on its photophysical properties, such as absorption and emission wavelengths and luminescence lifetimes. The obtained values indicate that the expansion of the 1,10-phenanthroline frame by phenyl and phenylacetylene leads to a lowering of the energies of the excited states. To further elucidate the influence of the substituents on the excited states of the corresponding complexes, detailed Raman spectroscopic investigations were performed.

Raman and Resonance Raman Spectroscopy

An extremely capable method of analysing the localisation of the ^{1}MLCT excited state is resonance Raman (rR) spectroscopy, which is an excellent tool to characterise the molecular degrees of freedom involved in the initial structural changes of photochemically active systems, e.g. to analyse the Franck–Condon point of an electronic transition.[44,45] It is important to consider the Franck–Condon point because the subsequent excited state relaxations will be initiated at this point. If the Raman excitation wavelength lies within the absorption band, the resonance condition is achieved and the vibrational modes, involved in the electronic transition, are selectively enhanced. The enhancement factor is about 10^6 relative to off-resonance measurements.[45] Therefore, rR spectroscopy is the method of choice of examining which particular ligand of the investigated heteroleptic ruthenium complexes is involved in the metal-to-ligand charge-transfer (^{1}MLCT) processes.[39,46–48]

Prior to resonance Raman spectroscopy, the analysis of the off-resonance Raman spectra is required to identify marker bands of the different ligands. This will facilitate the analysis of the rR data obtained for the complexes. Therefore, the solid-state Raman spectra of the complexes RuLR were compared with the Raman spectrum of $[Ru(tbbpy)_3]^{2+}$ (Figure 8). The Raman bands located in the range of the ring vibrations at 1617, 1541, 1483, 1420, 1372 and 1316 cm^{-1} of the homoleptic complex can clearly be assigned to the 4,4′-bis(*tert*-butyl)-2,2′-bipyridine (tbbpy) ligand. When this spectrum is compared with the Raman bands of Ru**L1**–Ru**L4**, differences are detected, and the new bands can be assigned to the different 1,10-phenanthroline ligands. However, a similarity between the Raman spectra of Ru**L1**–Ru**L4** is observed in this investigated range, which indicates that substitution at the 3,8 positions has only small influence on the vibrations of the 1,10-phenanthroline system. Some new Raman bands of Ru**L3** located at 1390 and 1001 cm^{-1} can be assigned to vibrations of the phenyl groups of the substituents. Furthermore, comparison of the spectra of Ru**L1** with Ru**L4** shows differences; some Raman bands of the substituent at 1578, 1147 and 999 cm^{-1} for the latter compound have a high intensity and thus change the appearance of the Raman spectrum. These Raman bands can be assigned to vibrations of the phenyl rings. In addition, the C≡C stretch vibration occurs at 2220 cm^{-1}.

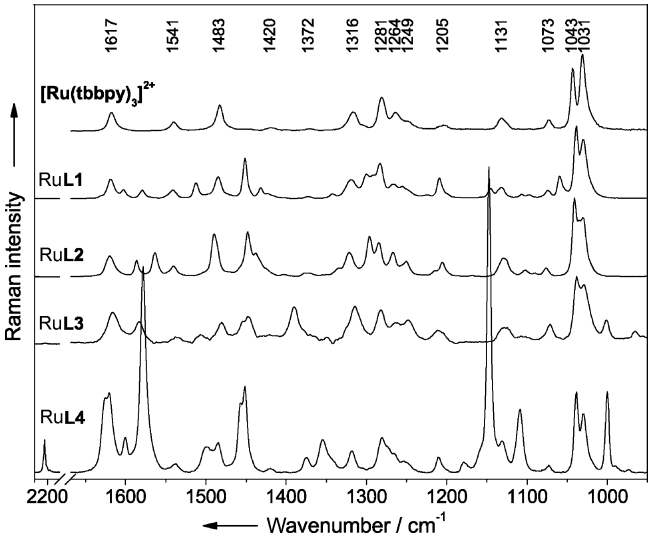

Figure 8. Off-resonance Raman spectra of Ru**L1**–Ru**L4** and $[Ru(tbbpy)_3]^{2+}$ in the solid state recorded at an excitation wavelength of 830 nm. The spectra are normalised to the band at 1031 cm^{-1}.

The localisation of the ^{1}MLCT excited state was investigated for the complexes Ru**L2**–Ru**L4**, dissolved in dichloromethane, with resonance Raman spectroscopy (Figure 9).

The resonance Raman spectrum of the homoleptic complex $[Ru(tbbpy)_3]^{2+}$, measured at an excitation wavelength of 458 nm, is displayed in Figure 9 for comparison and exhibits enhanced Raman bands located at the tbbpy ligand. The excitation wavelength of 488 nm for Ru**L4** lies within the first absorption band (Figure 5), and the obtained spectrum of Ru**L4** shows new bands that can clearly be associated with the newly introduced ligand **L4** by comparing them with the spectrum of $[Ru(tbbpy)_3]^{2+}$. The Raman bands located at 2220, 1625, 1576, 1497, 1449, 1373, 1352, 1208, 1146, 1111 and 999 cm^{-1} can be assigned to ^{1}MLCT processes to **L4** in Ru**L4**. Thus, an excitation of both ligands, tbbpy and **L4** is observable with excitation at 488 nm, and notably, the vibrational modes of the phenylacetylene substituent at 2220, 1576 and 999 cm^{-1} are involved. This is in contrast to the results from the rR investigations of the complex $[Ru(bpy)_2(phen)]^{2+}$, in which the ^{1}MLCT transition is favoured for the bpy ligand.[49] A similar localisation of the ^{1}MLCT process, in comparison to Ru**L4**, can be observed for Ru**L3**. For this compound, the rR spectra obtained at 488 nm show enhanced Raman bands of the two ligands tbbpy and **L3**.

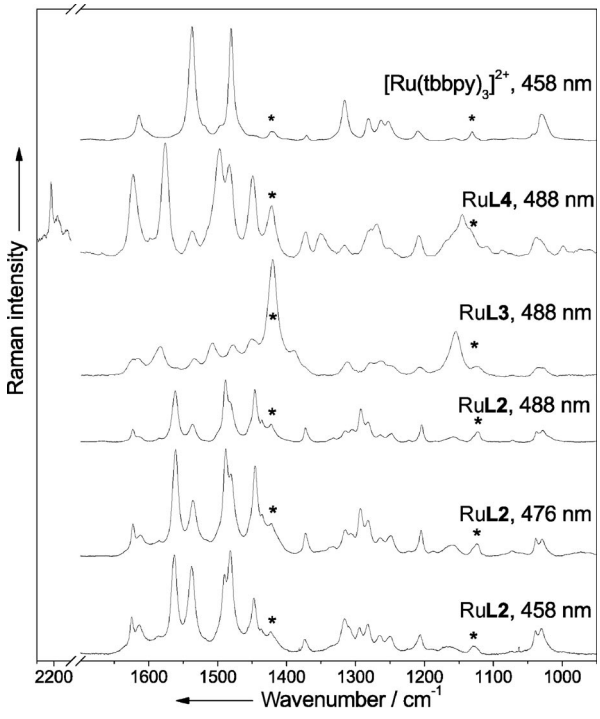

Figure 9. Resonance Raman spectra of Ru**L2**, Ru**L3**, Ru**L4** and, for comparison, of $[Ru(tbbpy)_3]^{2+}$ dissolved in dichloromethane (solvent bands are marked with *). The complexes were excited at different wavelengths lying within the first absorption band (Figure 7). The spectra of Ru**L2** are normalised to the solvent band at 702 cm^{-1}.

The rR spectra of complex Ru**L2** dissolved in dichloromethane were obtained by using excitation wavelengths of 488, 476 and 458 nm, which lie within the first absorption band (Figure 9). These spectra are normalised to the solvent band at 702 cm^{-1}. It can be seen that the spectrum at 488 nm shows enhanced Raman bands relative to the solvent band at 1423 cm^{-1}. The Raman bands located at 1624, 1562, 1489 and 1437 cm^{-1} can be associated to vibrations of **L2**. The remaining bands can be assigned to tbbpy. It is noticeable that the intensity of all Raman bands of the spectra measured at 458, 476 and 488 nm decrease with increasing excitation wavelength. The enhancement maximum for the Raman bands located at tbbpy seems to be at 458 nm, close to the absorption maximum of this complex (Figure 7, Table 3). In contrast, the Raman bands that can be assigned to **L2** show their maximum intensity at an excitation wavelength of 476 nm. Thus, resonance Raman spectroscopy shows that the lowest-energy absorption maximum can be assigned to a ^{1}MLCT process to the bromine-substituted phenanthroline **L2**.

Conclusions

The synthesis of ruthenium(II) complexes with regioselective functionalised 1,10-phenanthroline derivatives is facile and results in high yields of up to 95%. The 3,8-dibromine-substituted phenanthroline, **L2**, is easily transformed into the aryl-substituted phenanthroline by using organometallic Suzuki coupling with an optimised phosphane ligand system. The electrochemical investigations indicate that the new substituents at the phenanthroline ligands have a limited influence on the redox properties of the ruthenium centre, but a pronounced effect can be observed for the redox properties of the phenanthroline ligand. The photophysical data indicate that the newly introduced functionalities induce a bathochromic shift of the absorption and emission maxima of ligands and complexes alike. This general trend has been observed for the 3,5,6,8-tetrasubstituted phenanthroline complexes already.[12,14] On the basis of a comparison of these results, it is clear that substitution in the 5,6 positions in the latter complex has a far less pronounced effect on the photophysical properties of the corresponding complexes than substitution in the 3,8 positions. The resonance Raman investigation of the complexes shows that the tbbpy ligand and the substituted phenanthrolines are involved in the ^{1}MLCT transition. The detailed analysis of the data obtained for Ru**L2** shows that the lowest-energy section of the ^{1}MLCT band is increasingly localised on the bromine-substituted phenanthroline ligand. In general, the greater ease of reduction of the substituted phenanthrolines correlates quite well with their involvement in the ^{1}MLCT process. In conclusion, the results obtained indicate that bromine substitution at the 3 and 8 positions of 1,10-phenanthroline yields an excellent starting material for the synthesis of more extensive molecular structures that have different emission wavelengths and allow for the tuning of the localisation of the lowest-energy ^{1}MCLT level. From a synthetic point of view, it is very interesting that the introduction of bromine substituents alone is sufficient to induce some degree of directional electron transfer in the ^{1}MLCT state. This finding may form the basis for the development of photochemical molecular devices relying on directional energy or electron transfer.[1–3]

Experimental Section

If not stated otherwise, all Pd-catalysed cross-coupling reactions were conducted under argon or nitrogen by using standard Schlenk techniques. The Sonogashira[37] and Suzuki[33–36] reactions were carried out in anhydrous, freshly distilled solvents. Toluene and triethylamine were distilled from sodium benzophenone ketyl under argon prior to use. Methanol was dried with magnesium. All other solvents were of HPLC grade. 1,10-Phenanthroline monohydrate, phenylacetylene, 3,5-bis(trifluoromethyl)phenylboronic acid, NH_4PF_6 and all other materials were of commercial grade and used without further purification. $[Ru(tbbpy)_2Cl_2]$, 3,8-bis(phenylacetylene)-1,10-phenanthroline and S-Phos were prepared according to literature methods.[8,10,36,50]

^1H NMR and ^{13}C NMR spectra were recorded at ambient temperature on a Bruker AC 200 or AC 400 MHz spectrometer (^1H: 400.25 MHz, ^{13}C: 100.65 MHz). All spectra were referenced to tms or deuterated solvent as an internal standard (measured values for δ are given in ppm and for J in Hz). Mass spectra were performed on a Finnigan MAT SSQ 710 instrument at the Friedrich-Schiller University, Jena. UV/Vis spectra (accuracy ±2 nm) were obtained by using a Specord S600 from Analytik Jena. Emission spectra were measured at 298 K by using a Perkin–Elmer LS50B equipped with a Hamamatsu R928 red-sensitive detector. Quartz cells with a 10 mm pathlength were used for recording UV/Vis and emission spectra. Luminescence quantum yields were measured with diluted solutions (optical density < 0.05) with $[Ru(bpy)_3]Cl_2$ in nondegassed water (Φ = 0.028)[51] and quinine sulfate (Φ = 0.55) as references.

The microwave-assisted reactions were carried out by using the Microwave Laboratory Systems MLS EM-2 microwave system. Elemental analyses were performed by the Microanalytical Laboratory of the University Jena. For the sonication reaction, a Bandelin Sonorex Super RK 156 BH ultrasonic bath with a HF power of P = 150 W and a HF frequency f = 35 kHz was used.

Electrochemical data were obtained with cyclic voltammetry by using a conventional single-compartment, three-electrode cell arrangement in combination with a potentiostat "AUTOLAB®, Eco Chemie". A 0.196 cm^2 Pt disk was used as an auxiliary electrode, the working electrode was glassy carbon and the reference electrode Ag/AgCl (3 M KCl). The measurements were carried out in anhydrous and nitrogen-purged acetonitrile with 0.1 M terabutylammonium tetrafluoroborate as supporting electrolyte. All potentials are referenced by the ferrocenium/ferrocene couple [E(Fc/Fc$^+$) = 0.45 V].

Luminescence lifetime measurements were obtained by using an Edinburgh Analytical Instrument (EAI) time-correlated single-photon-counting apparatus (TCSPC) comprised of two model J-yA monochromators (emission and excitation), a single-photon-photomultiplier detection system model 5300 and a F900 nanosecond flashlamp (nitrogen filled at 1.1 atm pressure, 40 kHz or 0.3 atm pressure, 20 kHz) interfaced with a personal computer by a NorlandMCA card. A 410-nm cut-off filter was used for the emission measurements to attenuate scatter of the excitation light (337 nm); luminescence was monitored at the λ_{max} of the emission. Data correlation and manipulation was carried out by using EAI F900 software version 6.24. Emission lifetimes were calculated with a single-exponential fitting function, Levenberg–Marquardt algorithm with iterative deconvolution (Edinburgh instruments F900 software). The reduced χ^2 (<1.05) and residual plots were used to judge the quality of the fits. Lifetimes are ±5%.

The resonance Raman spectra were measured with a conventional 90°-scattering arrangement. The excitation lines at 488 and 458 nm provided by an argon ion laser (Modell Coherent Innova 300C MotoFreD Ion Laser) served as the resonant excitation in the range of the MLCT absorption band. A rotating cell was utilised to prevent the heating of the samples. No changes in the absorption spectra of the complexes could be observed after exposure to the resonant laser light. The scattered light was collected with a lens (f_1 = 35 mm) and subsequently focussed (f_2 = 50 mm) onto the entrance slit of an Acton SpectraPro 2758i spectrometer. The dispersed Raman stray light was detected with a CCD-camera from Princeton Instruments, labelled with a Spec-10 400B/LN back-illuminated CCD. The concentration of the solutions was optimised to obtain a maximum signal-to-noise ratio and was in the millimolar range.

Crystal-Structure Analyses: The structure determinations were carried out on an Enraf Nonius Kappa CCD diffractometer, by using graphite monochromated Mo-K_α radiation. The crystals were mounted in a stream of cold nitrogen, with a distance of 29 mm to the crystal detector. Data were corrected for Lorentz and polarisation effects but not for absorption.[52,53] The structures were solved by direct methods (SHELXS[54]) and refined by full-matrix least-squares techniques against F_o^2 (SHELXL-97[55]). The hydrogen atoms were included at calculated positions with fixed thermal parameters during the final stages of the refinement. All non-hydrogen atoms were refined anisotropically.[55] The molecular illustrations were drawn with the program XP (SIEMENS Analytical X-ray Instruments, Inc.). CCDC-676105 (**L2**), and CCDC-676106 (Ru**L2**) contains the supplementary crystallographic data for this paper. These data can be obtained free of charge from The Cambridge Crystallographic Data Centre via www.ccdc.cam.ac.uk/data_request/cif.

Crystal Data for phenBr_2 (L2): Crystals suitable for X-ray analysis were obtained from chloroform. $C_{12}H_6Br_2N_2{\cdot}CHCl_3$, M_r = 457.38 g mol^{-1}, colourless prism, size 0.04 × 0.04 × 0.03 mm, orthorhombic, space group *Pnma*, a = 21.149(4), b = 6.7797(14), c = 10.982(2) Å, V = 1574.6(6) Å^3, T = –90 °C, Z = 4, $\rho_{calcd.}$ = 1.929 g cm^{-3}, μ (Mo-K_α) = 56.46 cm^{-1}, F(000) = 880, 10336 reflections in h(–26/27), k(–8/8), l(–13/14), measured in the range 1.93° ≤ Θ ≤ 27.47°, completeness Θ_{max} = 99.9%, 1957 independent reflections, R_{int} = 0.0545, 1444 reflections with $F_o > 4\sigma(F_o)$, 118 parameters, 0 restraints, R_{1obs} = 0.0606, wR_{2obs} = 0.1596, R_{1all} = 0.0868, wR_{2all} = 0.1773, GOOF = 1.042, largest difference peak and hole 3.285/–1.082 e Å^{-3}.

Crystal Data for $[(tbbpy)_2Ru(phenBr_2)](PF_6)_2$ (RuL2): Crystals suitable for X-ray analysis were obtained from acetone/water. $C_{48}H_{54}Br_2F_{12}N_6P_2Ru{\cdot}1.25C_3H_6O{\cdot}0.5H_2O$, M_r = 1322.87 g mol^{-1}, red–brown prism, size 0.05 × 0.05 × 0.04 mm, triclinic, space group $P\bar{1}$, a = 16.6627(3), b = 19.7941(5), c = 19.9314(5) Å, α = 83.234(1), β = 65.869(1), γ = 81.967(1)°, V = 5927.1(2) Å^3, T = –90 °C, Z = 4, $\rho_{calcd.}$ = 1.482 g cm^{-3}, μ (Mo-K_α) = 17.45 cm^{-1}, F(000) = 2670, 42776 reflections in h(–21/21), k(–25/25), l(–25/23), measured in the range 2.69° ≤ Θ ≤ 27.46°, completeness Θ_{max} = 99.2%, 26922 independent reflections, R_{int} = 0.0346, 18497 reflections with $F_o > 4\sigma(F_o)$, 1252 parameters, 0 restraints, R_{1obs} = 0.0785, wR_{2obs} = 0.2096, R_{1all} = 0.1176, wR_{2all} = 0.2452, GOOF = 1.011, largest difference peak and hole 2.049/–2.074 e Å^{-3}.

Crystal Data for $[(tbbpy)_2Ru\{phen(tfmp)_2\}](PF_6)_2$ (RuL3): Crystals suitable for X-ray analysis were obtained from acetone/water. $C_{67}H_{66}F_{24}N_6OP_2Ru$, M_r = 1590.27 g mol^{-1}, red prism, size 0.38 × 0.10 × 0.01 mm, triclinic, space group $P\bar{1}$, a = 16.3058(2), b = 19.910(3), c = 24.570(3) Å, α = 94.772(7), β = 90.300(6), γ = 104.524(5)°, V = 7691.9(17) Å^3, Z = 4, $\rho_{calcd.}$ = 1.373 g cm^{-3}, μ (Mo-K_α) = 2.944 mm^{-1}, F(000) = 3232, 116847 reflections measured in the range 1.80° ≤ Θ ≤ 70.09°, 24257 independent reflec-

tions, 1823 parameters, R_{1obs} = 0.1908, wR_{2obs} = 0.4320, GOOF = 1.266, largest difference peak and hole 2.591/–1.102 e Å^{-3}.

3,8-Dibromo-1,10-phenanthroline (L2): For this synthesis a slightly modified literature procedure was used.[8] 1,10-Phenanthroline monohydrate was treated with Br_2 in the presence of S_2Cl_2 and pyridine to afford 3,8-dibromo-1,10-phenanthroline. The workup procedure was slightly modified relative to reported approaches. First, the crude product was purified with column chromatography (with silica and chloroform) and then recrystallised from a mixture of carbon tetrachloride and chloroform. At the end, a white powder was obtained. Yield: 6.01 g (64%). ^{1}H NMR ($CDCl_3$, 400 MHz): δ = 9.126 (d, J = 2.4 Hz, 2 H), 8.594 (d, J = 2.4 Hz, 2 H), 7.743 (s, 2 H) ppm. MS (DEI): m/z (%) = 338 (100) [M + H$^+$], 259 (65) [M – Br + H$^+$], 178 (34) [M – 2Br + H$^+$].

3,8-Bis[{3,5-bis(trifluoromethyl)}phenyl]-1,10-phenanthroline (L3): The catalytic reaction was run under a nitrogen atmosphere. 3,8-dibromo-1,10-phenanthroline (**L2**, 0.08 g, 0.24 mmol), 3,5-bis(trifluoromethyl)phenylboronic acid (0.13 g, 0.50 mmol), Cs_2CO_3 (3.2 g, 0.01 mol), S-Phos (6 mg, 0.014 mmol, 6 mol-%) were placed together into a Schlenk tube. Thereafter, freshly distilled tertrahydrofuran (70 mL) and deoxygenated water (5 mL) were added. The mixture was stirred and degassed with nitrogen for 30 min. After addition of $Pd_2(dba)_3$ (6 mg, 0.007 mmol, 3 mol-%), the yellow reaction mixture was heated at reflux under nitrogen for 3 d. The suspension was then cooled to room temperature, taken up into water and extracted with chloroform. The solvent of the combined organic layers was removed, and the crude product was dried under vacuum. The residue was cleaned by column chromatography by collecting the main fluorescent band (silica and chloroform). Yield: 0.14 g (95%). ^{1}H NMR ($CDCl_3$, 400 MHz): δ = 9.438 (d, J = 2.0 Hz, 2 H); 8.488 (d, J = 2.0 Hz, 2 H), 8.192 (m, 4 H), 7.990 (m, 4 H) ppm. ^{13}C NMR ($CDCl_3$, 100 MHz): δ = 120.10, 125.52, 127.26, 128.40, 132.18, 132.84, 133.12, 133.97, 139.37, 145.50, 148.64 ppm. MS (DEI): m/z (%) = 605 (100) [M + H$^+$], 302 (23) [M/2]$^{2+}$.

3,8-Bis(phenylacetylene)-1,10-phenanthroline (L4): The synthetic procedure used for 3,8-bis(phenylacetylene)-1,10-phenanthroline is based on the report by Tor et al., but was slightly changed.[10] The Pd-catalysed Sonogashira cross-coupling reactions were carried out under an argon atmosphere. Furthermore, the use of ultrasound and a temperature of 40 °C were necessary to introduce the alkyne functions. At first a standard Schlenk vessel was charged with 3,8-dibromo-1,10-phenanthroline (0.2 g, 0.59 mmol), $Pd(PPh_3)_2Cl_2$ (0.042 g, 0.06 mmol, 10.0 mol-%), copper iodide CuI (0.023 g, 0.12 mmol, 20.0 mol-%), methanol (12 mL) and dry triethylamine (18 mL). Finally, excess phenylacetylene (0.15 mL, 1.37 mmol) was added. The yellowish suspension was then sonicated at 40 °C under argon for 8 h. Thereafter, the reaction mixture was heated to 50 °C and stirred for 1 d. The suspension was then cooled to room temperature, taken up into an aqueous solution of potassium cyanide (0.02 g, 0.31 mmol) and dichloromethane. The water phase was well extracted with dichloromethane, and the solvent of the combined organic layers was removed. The crude product was then dried under vacuum. The residue was cleaned by column chromatography by collecting the main fluorescent band (silica and CH_2Cl_2/MeOH in a ratio of 20:1). Yield: 0.18 g (81%). ^{1}H NMR ($CDCl_3$, 400 Hz): δ = 9.283 (d, J = 1.6 Hz, 2 H), 8.390 (d, J = 2.0 Hz, 2 H), 7.803 (s, 2 H), 7.605 (m, 4 H), 7.393 (m, 6 H) ppm. ^{13}C NMR ($CDCl_3$, 100 MHz): δ = 30.89, 85.78, 94.90, 120.47, 122.13, 127.02, 128.33, 128.55, 129.22, 131.89, 138.76, 151.88 ppm. MS (DEI): m/z (%) = 380 (100) [M + H$^+$], 190 (8) [M/2]$^{2+}$.

Typical Procedure for Preparation of RuLR (R = 1, 2, 3, 4) from [(tbbpy)$_2$RuCl$_2$] (where tbbpy = 4,4′-di-*tert*-butyl-2,2′-bipyridine) and LR: All prepared complexes contain tbbpy to increase the solubility in less polar organic solvents and were prepared by using a somewhat modified standard procedure.[14,50] For the complexation reaction, [(tbbpy)$_2$RuCl$_2$] (0.05 g, 0.07 mmol) and the corresponding ligand **LR** (R = 1, 2, 3, 4; 0.07 mmol) were suspended in ethanol/water (50 mL/30 mL) and heated at reflux for 2 h with microwave irradiation (microwave setup: 30 s, 400 W; 2 h, 150 W, 10 min ventilation). After cooling to room temperature, the red solution was filtered, followed by evaporation of 90% of the solvent on the rotary evaporator. An aqueous solution of NH_4PF_6 was then added, and the precipitate was removed by filtration, washed with water and a small amount of EtOH and Et_2O and dried in air.

[(tbbpy)$_2$Ru(phenBr$_2$)](PF$_6$)$_2$ (RuL2): Yield: 0.08 g (91%). $C_{48}H_{54}Br_2F_{12}N_6P_2Ru$ (1265.80): calcd. C 43.00, H 4.33, N 6.69; found C 43.17, H 4.52, N 6.35. ^{1}H NMR ([D$_3$]CD$_3$CN, 400 MHz): δ = 8.805 (d, J = 1.6 Hz, 2 H), 8.486 (d, J = 1.6 Hz, 2 H), 8.452 (d, J = 1.6 Hz, 2 H), 8.173 (s, 2 H), 7.997 (d, J = 1.6 Hz, 2 H), 7.623 (d, J = 6.0 Hz, 2 H), 7.452 (dd, J = 5.6, 2.0 Hz 2 H), 7.437 (d, J = 6.0 Hz, 2 H), 7.215 (dd, J = 6.0, 2.0 Hz, 2 H), 1.438 (s, 18 H, *tert*-butyl), 1.379 (s, 18 H, *tert*-butyl) ppm. ^{13}C NMR ([D$_3$]CD$_3$CN, 100 MHz): δ = 30.43, 30.47, 36.27, 36.36, 122.04, 122.62, 125.34, 125.60, 129.36, 132.41, 139.57, 147.23, 152.23, 152.63, 154.23, 157.64, 158.10, 163.80, 163.92 ppm. MS (ESI in CH$_3$CN and MeOH): m/z (%) = 1121.1 (100) [M – 1PF$_6$]$^+$ with matching isotopic pattern, 487.8 (10) [M – 2PF$_6$/2]$^{2+}$ with matching isotopic pattern.

[(tbbpy)$_2$Ru{phen(tfmp)$_2$}](PF$_6$)$_2$ (RuL3): Yield: 0.08 g (74%). $C_{64}H_{60}F_{24}N_6P_2Ru{\cdot}1H_2O$: calcd. C 49.58, H 4.03, N 5.42; found C 49.11, H 3.82, N 5.31. ^{1}H NMR ([D$_3$]CD$_3$CN, 400 MHz): δ = 8.979 (d, J = 2.0 Hz, 2 H), 8.483 (d, J = 2.0 Hz, 2 H), 8.447 (d, J = 2.0 Hz, 2 H), 8.351 (s, 2 H), 8.155 (m, 4 H), 8.137 (d, J = 2.0 Hz, 2 H), 7.755 (d, J = 6.0 Hz, 2 H), 7.576 (d, J = 6.0 Hz 2 H), 7.479 (dd, J = 5.6, 1.6 Hz, 2 H), 7.229 (dd, J = 6.0, 2.0 Hz, 2 H), 1.399 (s, 18 H, *tert*-butyl), 1.338 (s, 18 H, *tert*-butyl) ppm. ^{13}C NMR ([D$_3$]CD$_3$CN, 100 MHz): δ = 30.41, 36.25, 36.33, 122.54, 122.67, 122.97, 123.94, 125.25, 125.39, 125.68, 129.38, 129.96, 131.96, 132.81, 133.15, 133.48, 135.97, 136.74, 139.08, 148.13, 151.86, 152.72, 157.86, 158.29, 163.57, 163.82 ppm. MS (ESI in CH$_3$CN and MeOH): m/z (%) = 1387.1 (29) [M – 1PF$_6$]$^+$ with matching isotopic pattern, 621.1 (100) [M – 2PF$_6$/2]$^{2+}$ with matching isotopic pattern.

[(tbbpy)$_2$Ru{phen(phac)$_2$}](PF$_6$)$_2$ (RuL4): Yield: 0.065 g (71%). $C_{64}H_{64}F_{12}N_6P_2Ru$ (1308.24): calcd. C 58.76, H 4.93, N 6.42; found C 58.98, H 4.45, N 6.24. ^{1}H NMR ([D$_3$]CD$_3$CN, 400 MHz): δ = 8.687 (d, J = 1.6 Hz, 2 H), 8.521 (d, J = 2.0 Hz, 2 H), 8.479 (d, J = 2.0 Hz, 2 H), 8.217 (s, 2 H), 8.060 (d, J = 2.0 Hz, 2 H), 7.700 (d, J = 6.0 Hz, 2 H), 7.541 (m, 10 H), 7.519 (d, J = 6.4 Hz, 2 H), 7.468 (dd, J = 6.4, 2.0 Hz, 2 H), 7.244 (dd; J = 6.0, 2.0 Hz, 2 H), 1.431 (s, 18 H, *tert*-butyl), 1.358 (s, 18 H, *tert*-butyl) ppm. ^{13}C NMR ([D$_3$]CD$_3$CN, 100 MHz): δ = 30.42, 30.49, 36.26, 36.37, 85.43, 96.61, 122.26, 122.59, 122.64, 123.33, 125.39, 125.66, 129.50, 129.89, 130.95, 131.58, 132.67, 139.11, 147.31, 152.22, 152.52, 154.84, 157.71, 158.13, 163.66, 163.76 ppm. MS (ESI in MeOH): m/z (%) = 1163.2 (100) [M – 1PF$_6$]$^+$ with matching isotopic pattern, 1017.2 (11) [M – 2PF$_6$ – H]$^+$ with matching isotopic pattern.

Acknowledgments

This work was financially supported by the Deutsche Forschungs gemeinschaft (DFG) and the Deutscher Akademischer Austausch Dienst (DAAD). D. C. and G. S. H. thank the Natural Sciences and Engineering Research Council of Canada (NSERC) and the

Université de Montréal. G. S. H. thanks the RSC for a Journals Grant for Authors. S. K. is very grateful to the Verband der Chemischen Industrie (VCI/FCI) for a Ph.D. grant.

[1] V. Balzani, A. Juris, M. Venturi, S. Campagna, S. Serroni, *Chem. Rev.* **1996**, *96*, 759–833.
[2] V. Balzani, M. Venturi, A. Credi, *Molecular Devices and Machines: A Journey into the Nano World*, Wiley-VCH, Weinheim, **2003**.
[3] N. D. McClenaghan, Y. Leydet, B. Maubert, M. T. Indelli, S. Campagna, *Coord. Chem. Rev.* **2005**, *249*, 1336–1350.
[4] J. G. Vos, J. M. Kelly, *Dalton Trans.* **2006**, 4869–4883.
[5] A. A. Schilt, W. E. Dunbar, *Tetrahedron* **1974**, *30*, 401–403.
[6] P. J. Giordano, C. R. Bock, M. S. Wrighton, *J. Am. Chem. Soc.* **1978**, *100*, 6960–6965.
[7] C. O. Dietrich-Buchecker, P. A. Marnot, J. P. Sauvage, *Tetrahedron Lett.* **1982**, *23*, 5291–5294.
[8] C. Dietrich-Buchecker, M. C. Jimenez, J. P. Sauvage, *Tetrahedron Lett.* **1999**, *40*, 3395–3396.
[9] D. Tzalis, Y. Tor, S. Failla, J. S. Siegel, *Tetrahedron Lett.* **1995**, *36*, 3489–3490.
[10] D. Tzalis, Y. Tor, *Tetrahedron Lett.* **1995**, *36*, 6017–6020.
[11] D. Tzalis, Y. Tor, *Angew. Chem. Int. Ed. Engl.* **1997**, *36*, 2666–2668.
[12] S. Rau, R. Fischer, M. Jäger, B. Schäfer, S. Meyer, G. Kreisel, H. Görls, M. Rudolf, W. Henry, J. G. Vos, *Eur. J. Inorg. Chem.* **2004**, 2001–2003.
[13] J. Frey, T. Kraus, V. Heitz, J. Sauvage, *Chem. Commun.* **2005**, 5310–5312.
[14] B. Schäfer, H. Görls, S. Meyer, W. Henry, J. G. Vos, S. Rau, *Eur. J. Inorg. Chem.* **2007**, 4056–4063.
[15] C. Goze, C. Sabatini, A. Barbieri, F. Barigelletti, R. Ziessel, *Eur. J. Inorg. Chem.* **2008**, 1293–1299.
[16] J. Bolger, A. Gourdon, E. Ishow, J. Launay, *Inorg. Chem.* **1996**, *35*, 2937–2944.
[17] R. Eisenberg, W. Paw, *Inorg. Chem.* **1997**, *36*, 2287–2293.
[18] N. Komatsuzaki, R. Katoh, Y. Himeda, H. Sugihara, H. Arakawa, K. Kasuga, *J. Chem. Soc., Dalton Trans.* **2000**, 3053–3054.
[19] S. Ott, R. Faust, *Synthesis* **2005**, 3135–3139.
[20] G. Conte, A. J. Bortoluzzi, H. Gallardo, *Synthesis* **2006**, 3945–3947.
[21] A. K. Mesmaeker, G. Orellana, J. K. Barton, N. J. Turro, *Photochem. Photobiol.* **1990**, *52*, 461–472.
[22] M. T. Mongelli, J. Heinecke, S. Mayfield, B. Okyere, B. S. J. Winkel, K. J. Brewer, *J. Inorg. Biochem.* **2006**, *100*, 1983–1987.
[23] H. Ozawa, M. Haga, K. Sakai, *J. Am. Chem. Soc.* **2006**, *128*, 4926–4927.
[24] H. Ozawa, K. Sakai, *Chem. Lett.* **2007**, *36*, 920–921.
[25] S. Rau, B. Schäfer, D. Gleich, E. Anders, M. Rudolph, M. Friedrich, H. Görls, W. Henry, J. G. Vos, *Angew. Chem. Int. Ed.* **2006**, *45*, 6215–6218.
[26] S. Rau, D. Walther, J. G. Vos, *Dalton Trans.* **2007**, 915–919.
[27] A. Fihri, V. Artero, M. Razavet, C. Baffert, W. Leibl, M. Fontecave, *Angew. Chem. Int. Ed.* **2008**, *47*, 564–567.
[28] J. C. Chambron, J. P. Sauvage, *Tetrahedron Lett.* **1986**, *27*, 865–868.
[29] J. Frey, C. Tock, J. Collin, V. Heitz, J.-P. Sauvage, K. Rissanen, *J. Am. Chem. Soc.* **2008**, *130*, 11013–11022.
[30] P. J. Connors Jr, D. Tzalis, A. L. Dunnick, Y. Tor, *Inorg. Chem.* **1998**, *37*, 1121–1123.
[31] B. D. MacCraith, C. M. McDonagh, G. O'Keeffe, T. E. Keyes, J. G. Vos, B. O'Kelly, J. F. McGilp, *Analyst* **1993**, *118*, 385–388.
[32] M. Schmittel, H. Ammon, *Eur. J. Org. Chem.* **1998**, 785–792.
[33] A. Suzuki, *Pure Appl. Chem.* **1985**, *57*, 1749–1758.
[34] A. Suzuki, *Pure Appl. Chem.* **1991**, *63*, 419–422.
[35] W. Frank, T. Pautzsch, E. Klemm, *Macromol. Chem. Phys.* **2001**, *202*, 2535–2537.
[36] T. E. Barder, S. D. Walker, J. R. Martinelli, S. L. Buchwald, *J. Am. Chem. Soc.* **2005**, *127*, 4685–4696.
[37] K. Sonogashira in: *Handbook of Organopalladium Chemistry for Organic Synthesis*, John Wiley & Sons, **2002**, vol. 1, p. 493–529.
[38] D. J. Hurley, J. R. Roppe, Y. Tor, *Chem. Commun.* **1999**, 993–994.
[39] M. Schwalbe, B. Schäfer, H. Görls, S. Rau, S. Tschierlei, M. Schmitt, J. Popp, G. Vaughan, W. Henry, J. G. Vos, *Eur. J. Inorg. Chem.* **2008**, 3310–3319.
[40] S. Campagna, F. Puntoriero, F. Nastasi, G. Bergamini, V. Balzani in *Topics in Current Chemistry: Photochemistry and Photophysics Of Coordination Compounds I* **2007**, 280, 117–214.
[41] S. Rau, K. Lamm, H. Görls, J. Schöffel, D. Walther, *J. Organomet. Chem.* **2004**, *689*, 3582–3592.
[42] J. Yang, A. Dass, C. Sotiriou-Leventis, D. S. Tyson, N. Leventis, *Inorg. Chim. Acta* **2005**, *358*, 389–395.
[43] E. C. Glazer, D. Magde, Y. Tor, *J. Am. Chem. Soc.* **2007**, *129*, 8544–8551.
[44] A. B. Myers, *Chem. Rev.* **1996**, *96*, 911–926.
[45] J. L. McHale in *Handbook of Vibrational Spectroscopy*, Wiley, New York **2002**, vol. 1, and references therein.
[46] S. Tschierlei, B. Dietzek, M. Karnahl, S. Rau, F. M. MacDonnell, M. Schmitt, J. Popp, *J. Raman Spectrosc.* **2008**, *39*, 557–559.
[47] B. Schäfer, H. Görls, M. Presselt, M. Schmitt, J. Popp, W. Henry, J. G. Vos, S. Rau, *Dalton Trans.* **2006**, 2225–2231.
[48] C. Hermann, J. Neugebauer, M. Presselt, U. Uhlemann, M. Schmitt, S. Rau, J. Popp, M. Reiher, *J. Phys. Chem. B* **2007**, *111*, 6078–6087
[49] C. V. Kumar, J. K. Barton, I. R. Gould, N. J. Turro, J. V. Houten, *Inorg. Chem.* **1988**, *27*, 648–651.
[50] S. Rau, B. Schäfer, A. Grüßing, S. Schebesta, K. Lamm, J. Vieth, H. Görls, D. Walther, M. Rudolph, U. W. Grummt, E. Birkner, *Inorg. Chim. Acta* **2004**, *357*, 4496–4503.
[51] K. Nakamura, *Bull. Chem. Soc. Jpn.* **1982**, *55*, 2697–2705.
[52] *COLLECT*, Data Collection Software, Nonius B. V., Netherlands, **1998**.
[53] Z. Otwinowski, W. Minor, *Methods Enzymol.* **1997**, *276*, 307–326.
[54] G. M. Sheldrick, *Acta Crystallogr., Sect. A* **1990**, *46*, 467–473.
[55] G. M. Sheldrick, *SHELXL-97*, University of Göttingen, Germany, **1997**

Received: April 3, 2009
Published Online: October 13, 2009

